Coupled reactors analysis: New needs and advances using Monte Carlo methodology

CrossMark

M. Aufiero [a], G. Palmiotti [b,*], M. Salvatores [b], S. Sen [b]

[a] University of California, Berkeley, Department of Nuclear Engineering, Berkeley, CA 94720-1730, USA
[b] NSDA Division, Idaho National Laboratory, P.O. Box 1625, Idaho Falls, ID 83415-3860, USA

ARTICLE INFO

ABSTRACT

Coupled reactors and the coupling features of large or heterogeneous core reactors can be investigated with the Avery's theory; however, the complex geometries that are often encountered in association with coupled reactors, require a detailed geometry description that can be easily provided by modern Monte Carlo (MC) codes. The results presented in this paper show that the MC code SERPENT has been successfully modified in order to compute the needed quantities like coupling coefficients. Moreover, the capability for calculating sensitivities to the quantities of interest for coupling reactors has been developed and implemented in SERPENT.

© 2016 Elsevier Ltd. All rights reserved.

1. Introduction

The idea of "coupled" reactors, i.e. reactors with e.g. two core regions with different spectra, neutronically coupled with or w/o a geometrical barrier (intermediate zone or buffer, more often without fissile material), has been originally proposed by Avery (1958). The motivation at the time was to couple a fast and a thermal assembly in order to obtain a combined system that can have the breeding ratio characteristics of an all-fast spectrum system and at the same time exhibiting a prompt neutron lifetime characteristic of a thermal neutron system, i.e. much higher than the one for an all-fast neutron system, considered at the time as a potential drawback.

The principle was experimentally tested (Toppel, 1957). Successively the fast-thermal coupling was often used to build fast neutron experimental facilities with a limited all-fast neutron zone (see for example Meister et al., 1964, and Bustraan et al., 1970); moreover that type of system was also experimentally realized e.g. in order to test the principle of specific coupled systems, as the pulse coupled reactor system consisting of fast burst reactor and a subcritical thermal module (Kukharchuk et al., 2000) or even a cluster of rocket reactors (Seale, 1964).

More recently, the potential of a coupled Fast-thermal reactor as versatile test reactor has been pointed out (Sen et al., 2016).

Theoretical methods have been developed to describe these systems both in steady and in transient conditions (see e.g. Avery, 1958; Baldwin, 1959; Komata, 1969; Abramov, 2001).

The "decoupling" of spatial regions in a reactor, is a well-recognized phenomenon that has been pointed out the early reactor physics studies. The decoupling/coupling effects are physics effects that can be found not only in the type of coupled systems mentioned above, but also in large reactors, where spatial regions can act as regions weakly or more strongly coupled. The potential flux tiltiness in the system can be associated for example to the so-called Boltzmann operator eigenvalue separation (see e.g. Abramov, 2001,) or, in case of a coupled system, the "flux tilting" between e.g. two regions, associated to the flux ratio in these regions, can be directly related to the ratio of the sub-criticality in the two regions (Seale, 1964).

In all cases, the performance analysis of these systems, both in steady or in transient conditions, requires a deep understanding of the, sometime non-conventional, physics phenomena, from the appropriate preparation of cross-sections to the evaluation of the impact of uncertainties and e.g. of the dependence of the specific coupling phenomena from nuclear data uncertainties.

Moreover, the detailed description of the geometry of typical coupled systems requires an appropriate Monte Carlo treatment; see e.g. Fig. 1 from Sen et al. (2016):

The need of using a Monte Carlo code implies its extension to the evaluation of the typical coupling parameters (see next section) and the development of a full sensitivity analysis capability. This capability should go beyond the standard reactor integral

* Corresponding author.
E-mail address: Giuseppe.Palmiotti@inl.gov (G. Palmiotti).

parameter sensitivity, but should be extended to coupling features of the system, kinetic parameters and spatial power distributions.

In this paper we will describe the theoretical formulations that have been developed for this purpose and their practical implementation together with some significant applications.

2. Short summary of some specific features of the Avery's theory

For the purpose of this paper, we will remind shortly the simplest form of the coupled reactor reactivity and criticality conditions that are given by (in the case of two coupled "regions", (see Avery, 1958)) for the coupling coefficients k_{ij}:

$$\begin{vmatrix} (k_{11} - 1) & k_{12} \\ k_{21} & (k_{22} - 1) \end{vmatrix} = 0, \tag{1}$$

$$k_{12}k_{21} = \Delta_1\Delta_2. \tag{2}$$

where ρ

$$\Delta_j = 1 - k_{jj} \tag{3}$$

If we indicate with S_i the power of region i, the power ratio in the two coupled regions is given by:

$$\frac{S_1}{S_2} = \frac{k_{12}}{\Delta_1} = \frac{\Delta_2}{k_{21}}. \tag{4}$$

In the general case of N regions one has to solve the following system:

$$\begin{pmatrix} k_{11}k_{12}\ldots k_{1N} \\ k_{21}k_{22}\ldots k_{2N} \\ \ldots \\ \ldots \\ \ldots \\ k_{N1}k_{N2}\ldots k_{NN} \end{pmatrix} \begin{pmatrix} S_1 \\ S_2 \\ . \\ . \\ . \\ S_N \end{pmatrix} = k \begin{pmatrix} S_1 \\ S_2 \\ . \\ . \\ . \\ S_N \end{pmatrix} \tag{5}$$

The reactivity ρ is defined as:

$$\rho \approx \sum_{i=1}^{N} \propto_i \frac{\delta v_i}{v_i}, \tag{6}$$

where

$$\propto_i = \frac{\frac{1}{\Delta_i}}{\sum_{j=1}^{N} \frac{1}{\Delta_j}} \tag{7}$$

The point kinetics equations are given (using exactly the same notations as in Avery (1958)) by:

$$l_{jk}\frac{dS_{jk}}{dt} = k_{jk}(1 - \beta)\sum_{m=1}^{N} S_{km} - S_{jk} + k_{jk}\sum_{i=1}^{D} \lambda_i C_{ki} \tag{8}$$

$$\frac{dC_{ki}}{dt} = \beta_i \sum_{m=1}^{N} S_{km} - \lambda_i C_{ki}. \tag{9}$$

where D is the number of delayed neutron families.

The power in region k is given by:

$$S_k = \sum_{m=1}^{N} S_{km} \tag{10}$$

In practice, the following expressions are the solution of the standard Boltzmann equations and that account for the space and energy dependence:

$$S_j = \int [v\sigma_f(r, v)]_j \varphi(r, v) dr dv. \tag{11}$$

$$S_{jk} = \frac{\int [v\sigma_f(r, v)]_j \varphi(r, v) dr dv \times \int \chi(v')\varphi^*(r, v')[v\sigma_f(r, v)]_j \varphi_k(r, v) dr dv dv'}{\int \chi(v')\varphi^*(r, v')[v\sigma_f(r, v)]_j \varphi(r, v) dr dv dv'} \tag{12}$$

$$k_{jk} = \frac{S_{jk}}{S_k} \tag{13}$$

$$k_{jk} = \frac{\int [v\sigma_f(r, v)]_j \varphi(r, v) dr, dv}{\int [v\sigma_f(r, v)]_k \varphi(r, v) dr dv}$$
$$\times \frac{\int \chi(v')\varphi^*(r, v')[v\sigma_f(r, v)]_j \varphi_k(r, v) dr dv dv'}{\int \chi(v')\varphi^*(r, v')[v\sigma_f(r, v)]_j \varphi(r, v) dr dv dv'}. \tag{14}$$

Using these expressions, one can solve the kinetics equations given above accounting for the energy and the within-region space dependence.

It has been shown the overall Avery formulation as indicated above, is well suited for a rather quick analysis not only of coupled systems of the type shown in Fig. 1, but also for the analysis of a wider class of systems of current interest. This is the case of the coupling of different regions in large, potentially decoupled systems like the proposed axially heterogeneous fast reactor ASTRID (Varaine et al., 2012), as shown in a simplified model below (Fig. 2), where the fertile region in the middle of the core can induce weak coupling effects among the different core regions:

In fact the k_{ij} coefficients give a rather accurate description of the coupling mechanism between core regions and the power evolution by region gives a first quantitative indication of potential power "tiltness" e.g. in case of asymmetrical reactivity insertion (Palmiotti and Salvatores, 2016).

3. Monte Carlo estimators for the coupled system parameters k_{ij} and l_{ij}

k_{ij} is defined as the average number of fission neutrons produced in the reactor i by a neutron born in the reactor j. Implicit Monte Carlo estimators for these quantities were implemented in several codes, in which the (spatially discretized) Fission Matrix
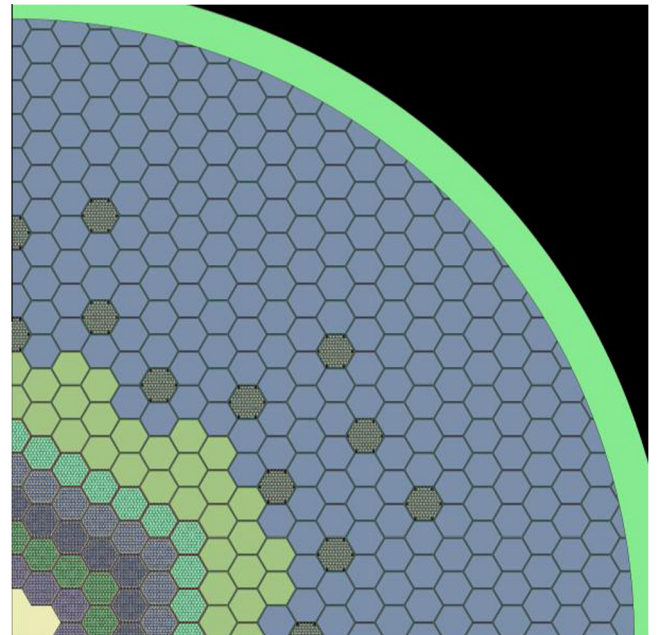

Fig. 1. XY view of a coupled thermal-fast irradiation test reactor (VCTR from Sen et al., 2016).
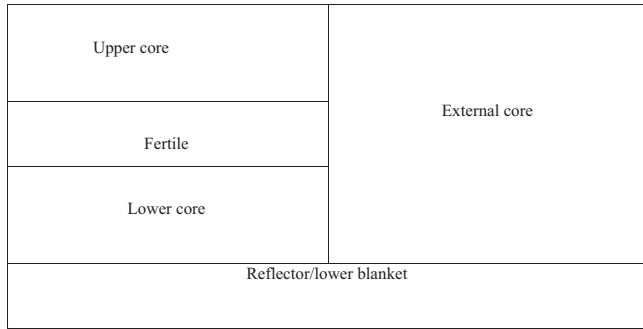
Fig. 2. ASTRID simplified model.

is scored (Carney et al., 2012). In this work, simple analog Monte Carlo estimators were preferred. This simplifies the implementation of the required adjoint-weighted calculation for the effective lives (l_{ij}) and the sensitivity coefficients (see next section). In particular, the calculation of k_{ij} involves the scoring of s_j and p_{ij}. The first quantity represents the total weight of the source neutrons from the reactor j in the present generation. This quantity is scored at the beginning of each Monte Carlo active cycle, checking the initial position of the source particles forming the whole neutron population:

$$s_j = \sum_{n \in j} w_n \tag{15}$$

w_n represents the weight of the generic particle n. In case of analog Monte Carlo transport, all the particles have the same weight.

Moreover, a label is attached to each particle, to save the ID of the reactor j of origin. A score w_n is added to the buffer p_{ij} every time a new fission neutron is produced in i from a neutron labeled j:

$$p_{ij} = \sum_{n \in (i \leftarrow j)} w_n \tag{16}$$

If N is the total number of reactors in the system, NxN p_{ij} buffers need to be allocated.

Estimates of the expected value for k_{ij} are produced at the end of each cycle as the ratios of the p_{ij} and $\pmb{s_j}$ scores:

$$k_{ij} \sim \tilde{k}_{ij} = \frac{E[p_{ij}]}{E[s_j]} \tag{17}$$

Statistical errors estimates for k_{ij} and the other quantities presented in the following are obtained by comparing the results obtained from different cycles, as common in Monte Carlo codes:

$$Var(k_{ij}) \sim E[(k_{ij})^2] - (E[k_{ij}])^2 \tag{18}$$

$E[(k_{ij})^2]$ represents the average of the squared k_{ij} estimates over a large number of cycles.

l_{ij} represents the effective prompt lifetime associated to the quantity k_{ij}. It can be view as the average lifetime of the neutrons born in j, producing a fission in i, weighted with the importance of the neutron. In cite (Laureau et al., 2015) the temporal aspect is introduced in the fission matrix approach by calculating the simple average time (i.e., not adjoint weighted) required by a neutron from j to produce a fission in i. In this work, the importance weighting was introduced adopting the Iterated Fission Probability (IFP) capabilities available in SERPENT (Leppänen et al., 2014):

$$l_{ij} = \frac{\sum_{n \in (j \leftarrow i)} w_n l_n I_n^g}{\sum_{n \in (j \leftarrow i)} w_n I_n^g} \tag{19}$$

where the sums are performed over all the neutrons in the population labeled with an origin in the reactor j and producing a fission in i. w_n is the weight of the neutron n and l_n is the associated lifetime. The Iterated Fission Probability approach estimates the importance of a particle through its contribution to the asymptotic neutron population. In particular, the expected importance of the neutron ($I_n^{(g)}$) is evaluated as the sum of the weights w_k of the descendants k of the neutron n, produced after g generations, normalized to the initial weight w_n:

$$I_n^{(g)} \sim \widetilde{I_n^{(g)}} \propto \frac{1}{w_n} \sum_{k \in d_n^{(g)}} w_k \tag{20}$$

The sum is performed over the set $d_n^{(g)}$ of the descendants.

Following the previous IFP implementation in SERPENT, adjoint weighted l_{ij} estimators are scored on each cycle computing the average lifetime of the gth ancestors that originated in j and produced a fission in i, over the present neutron population. This requires the additional propagation of the labels indicating the origin reactor j from each particle to the descendant (see Leppänen et al., 2014, for the details of the SERPENT IFP implementation).

4. Monte Carlo calculation of sensitivity coefficients for k_{ij}, l_{ij}

In this work, the collision history approach to Generalized Perturbation Theory (GPT) calculation previously implemented in SERPENT (Aufiero et al., 2015) was extended and adopted to estimate sensitivity coefficients involving k_{ij} and l_{ij} as response functions. The sensitivity coefficient $S_x^{k_{ij}}$ is defined as the relative change in k_{ij} the due to a perturbation in the generic parameter x. It represents the change in the probability of a neutron originated in j to produce a fission in i. The formulation introduced by Avery allows the fission rates in different reactors ($S_1, S_2 \ldots S_N$) to be derived from the matrix of the k_{ij} parameters. For this reason, the effects of perturbations in the system on k_{ij} are of particular interest in predicting and understanding the behavior of power distribution in coupled reactors.

The present investigation was focused on the evaluation of sensitivities involving perturbations in material compositions. This GPT approach estimates the sensitivity of a generalized response R to the atomic density of an isotope x from the correlation between the Monte Carlo scores for R and the accepted/rejected neutron collisions on x. In case of homogeneous problems (i.e., criticality source simulations), R is required to be in the form of the ratio of two quantities:

$$R = \frac{E[e_1]}{E[e_2]} \tag{21}$$

where $E[e_1]$ and $E[e_1]$ are the expected value for the Monte Carlo estimators related to the generic quantities e_1 and e_2. These estimators are usually obtained from the sum of analog or implicit scores over the neutron population, at each generation.

In analog Monte Carlo transport, changes in the considered parameters (e.g., reaction cross sections or material densities) lead to different paths of the particles, with respect to the reference, unperturbed system. The collision history-based approach to GPT calculations adopts a particle weight perturbation technique. This way, both in the perturbed and unperturbed systems the neutron population undergoes the same event chains. Nonetheless, the effect of parameters perturbations is accounted for by changing the weights of the particles. In case of first-order analysis, the weight perturbation of a particle is related to number of the past collision events involving the perturbed parameter x.

This weight perturbation approach allows the derivatives of the generic quantities e_1 and e_2 to be estimated from the correlation

between the particle collision events and the contribution of each particle to the scores for $E[e_1]$ and $E[e_2]$.

Usually, R is defined as the ratio of the integrals of two linear functions of the forward flux:

$$R = \frac{\langle \Sigma_1, \varphi \rangle}{\langle \Sigma_2, \varphi \rangle} \qquad (22)$$

or bi-linear functions of the forward and adjoint flux:

$$R = \frac{\langle \varphi^*, \Sigma_1 \varphi \rangle}{\langle \varphi^*, \Sigma_2 \varphi \rangle} \qquad (23)$$

In case of $R = k_{ij}$, the Monte Carlo estimator is implemented as the ratio of s_j and p_{ij} (see previous section).

The sensitivity coefficient S_{xij}^k is obtained as:

$$S_x^{kij} \sim \widetilde{S}_x^{kij} = \frac{COV[p_{ij}, \sum history(ACC_x - REJ_x)]}{E[p_{ij}]} - \frac{COV[s_j, \sum history(ACC_x - REJ_x)]}{E[s_j]} \qquad (24)$$

where $COV[p_{ij}, SUM (ACC_x {}_- REJ_x)]$ and $COV[p_{ij}, SUM (ACC_x {}_- REJ_x)]$ are the correlations between the scores of the Monte Carlo estimators for p_{ij} s_j, and the accepted/rejected collisions on the isotope $\mathbf{x}$, calculated over the whole neutron population. The sum is performed over the collision history buffer of each particle, to correctly take into account the effect of the perturbation on the fission source distribution (see Aufiero et al., 2015) $E[p_{ij}]$ $E[s_j]$ are the expected value for p_{ij} s_j. Monte Carlo estimators for these quantities were presented above.

A similar approach has been adopted to calculate sensitivity coefficients for l_{ij}. In this case, the denominator term of the response function is the adjoint-weighted sum of the weights of the neutrons originated in j, that produce a fission in i. The numerator term is the adjoint-weighted sum of the neutron lifetimes involved in this process. The calculation of sensitivities for the power distribution (S_1/S_2) makes use of the available GPT capabilities in the extended SERPENT version. S_1/S_2 is defined as:

$$\frac{S_1}{S_2} = \frac{\langle \Sigma_{f1}, \varphi \rangle}{\langle \Sigma_{f2}, \varphi \rangle} \qquad (25)$$

The spatial integrations are performed over the two reactors.

The current collision history-based implementation produces unbiased estimates for the indirect components of the effect of a perturbation (i.e., effects due to the modification of the flux φ):

$$\frac{\langle \Sigma_{f1}, \frac{\partial \varphi}{\partial x} \rangle}{\langle \Sigma_{f1}, \varphi \rangle} - \frac{\langle \Sigma_{f1}, \frac{\partial \varphi}{\partial x} \rangle}{\langle \Sigma_{f1}, \varphi \rangle} \qquad (26)$$

The direct component of the perturbation:

$$\frac{\langle \frac{\partial \Sigma_{f1}}{\partial x}, \varphi \rangle}{\langle \sum_{f1}, \varphi \rangle} - \frac{\langle \frac{\partial \Sigma_{f2}}{\partial x}, \varphi \rangle}{\langle \Sigma_{f2}, \varphi \rangle} \qquad (27)$$

is estimated separately (when present) via collisional detectors in an independent standard SERPENT calculation.

5. Verification and comparison against deterministic methodology

In order to verify the accuracy of the sensitivity Monte Carlo estimators presented above, a simple case study has been selected to test the GPT estimates against direct perturbation and ERANOS (Rimpault et al., 2002) reference results. Continuous-energy Monte Carlo results were obtained with Serpent, adopting the ENDF/B-VII nuclear data library. The case study consists in the spherical "coupled" system represented in Fig. 3.

The central region ("fast reactor") consists in a 9 cm sphere of a (30–70%) mixture of metallic ^{239}Pu and ^{238}U. The "thermal reactor" is made of a 9 cm thick spherical region of a water solution of ^{235}U (5.9 w%). The two regions are separated by a 1-cm thick boron carbide filter, to prevent the thermal neutrons from inducing fissions in the fast reactor. A graphite reflector surrounds the whole system. Fig. 4 shows the radial neutron flux distribution in the systems, divided in three energy groups: E > 0.1 MeV, 0.1 keV < E < 0.1 MeV and E < 0.1 keV.

The curves were obtained via standard collisional detector mesh in SERPENT, and show how the fast flux is highly peaked in the central region, whereas the low-energy flux is peaked in the center of the thermal region. Fig. 5 shows the fission rate weighted spectra in the two reactors.

The reference values for the Avery's coupling coefficients obtained with the Monte Carlo estimators presented above are reported in Table 1, and compared to ERANOS deterministic calculations. The subscripts 1 and 2 refer to the fast and thermal reactors, respectively.

The results of Table 1 show that both "reactors" present separately an effective multiplication factor around 0.8. The neutronic coupling between the two regions is strongly asymmetric: the values of k_{12} and k_{21} confirm the filtering effect of the boron carbide layer in limiting the probability for neutrons produced in the thermal reactor to produce fission in the central region. On the other hand, neutrons produced in the fast reactor present a large probability to cross the filter region and induce a fission in the thermal reactor.

SERPENT results appear in fairly good agreement with ERANOS values, confirming the consistency of the implemented estimators. For the verification of the sensitivity/perturbation calculations against direct perturbation results, the atomic density of H in the thermal reactor and ^{10}B in the filter region were changed by 5%. Independent Monte Carlo criticality source simulations were performed, adopting 10×10^9 for both the reference and the perturbed cases. In this way, the sensitivities of k_{ij}, l_{ij} and S1/S2 were accurately obtained via numerical differentiation, and compared to the GPT estimates.

The comparisons are presented in Tables 2 and 3. Results are expressed as sensitivity coefficients (relative values of $(\delta R/R)/(d\sigma/\sigma)$), where R is the integral parameter and σ the variable). The non-linear errors introduced by the finite
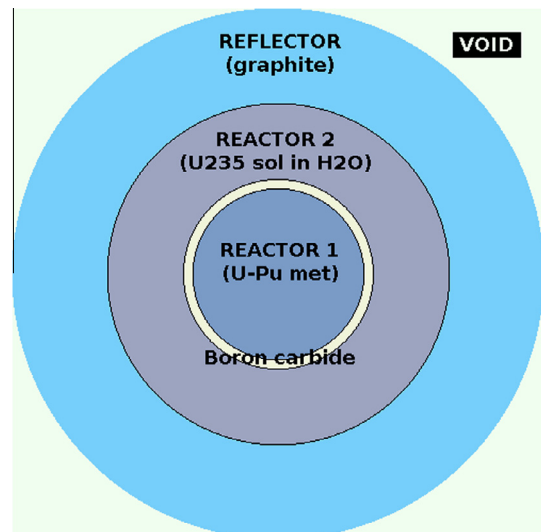

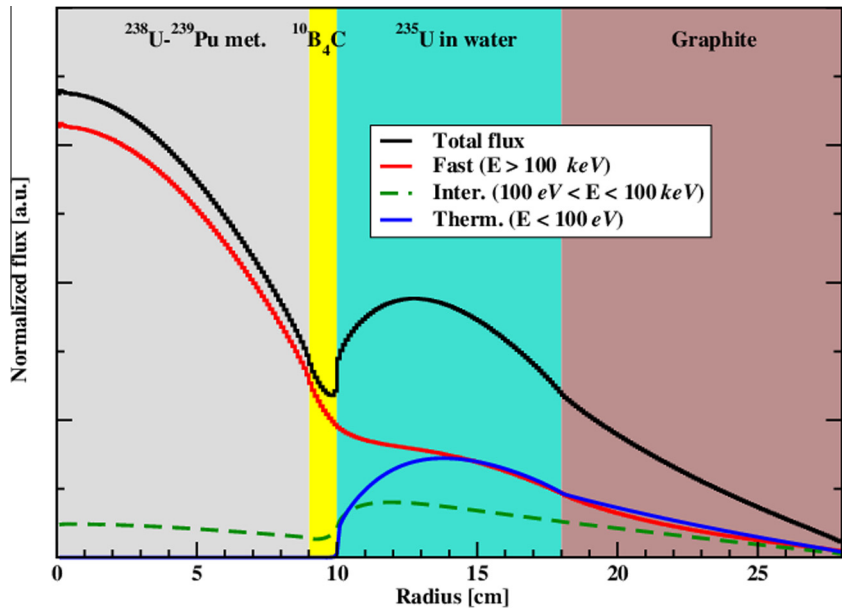**Fig. 3.** Simple model for verification calculations.

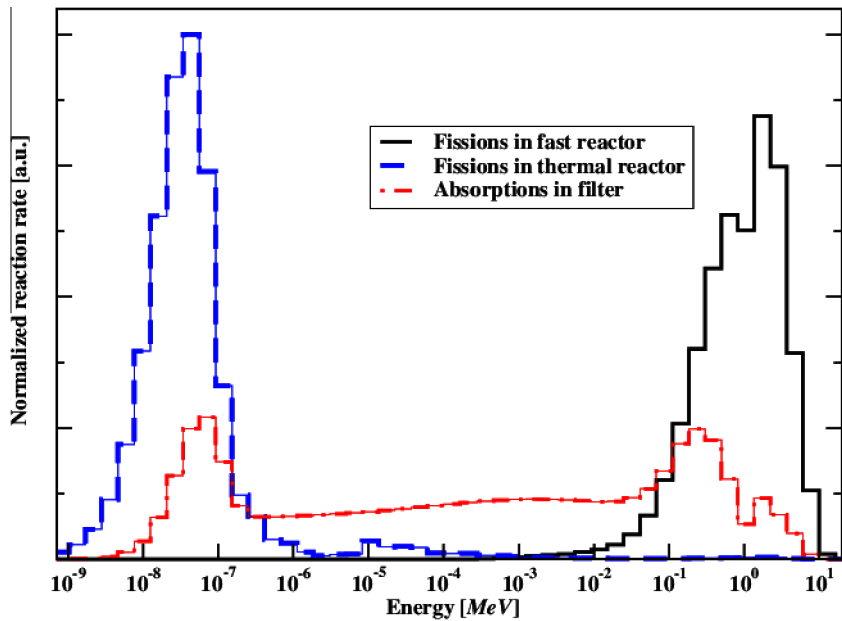**Fig. 4.** Radial neutron flux distribution in the simple model (three energy groups).

Fig. 5. Fission rate weighted spectra in the two reactors of the simple model.

Table 1
Comparison of coupling coefficients and neutron prompt lifetimes between SERPENT and ERANOS.

Parameter	SERPENT		ERANOS	Rel. diff.
	Value	Uncertainty (STD)		
k_{eff} all system	1.00074	±10 pcm (abs)	1.00031	0.04%
l_{eff} all system	18.37 µs	±0.1% (rel)	17.69 µs	3.8%
k_{11}	0.80023	±25 pcm (abs)	0.82576	−3.1%
k_{12}	0.07115	±5 pcm (abs)	0.078126	−8.9%
k_{21}	0.55199	±20 pcm (abs)	0.56959	−3.1%
k_{22}	0.80418	±13 pcm (abs)	0.80254	0.2%
l_{11}	9.11 ns	±0.2% (rel)	10.41 ns	−12.5%
l_{12}	20.97 ns	±0.3% (rel)	20.21 ns	3.8%
l_{21}	35.86 µs	±0.3% (rel)	35.17 µs	2.0%
l_{22}	38.69 µs	±0.1% (rel)	37.82 µs	2.3%

Table 2
Sensitivity coefficients to hydrogen density via perturbation theory and direct calculations.

Parameter	GPT	Direct pert.	Rel. diff. (%)	Uncertainty (rel. STD%)
k_{11}	−0.031	−0.028	−8.6	4.0
k_{12}	0.341	0.337	−1.0	0.5
k_{21}	−0.559	−0.551	−1.5	0.7
k_{22}	0.453	0.453	0.0	0.2
l_{11}	−0.041	−0.050	22.9	13.4
l_{12}	−0.367	−0.367	−0.1	2.8
l_{21}	−0.268	−0.252	−6.0	4.9
l_{22}	−0.255	−0.250	−2.3	2.4

Table 3
Sensitivity to ^{10}B density via perturbation theory and direct calculations.

Parameter	GPT	Direct pert.	Rel. diff. (%)	Uncertainty (rel. STD%)
k_{11}	0.027	−0.027	3.0%	0.7%
k_{21}	−0.197	−0.198	0.3%	0.1%
k_{12}	−0.221	−0.220	−0.5%	0.2%
k_{22}	−0.023	−0.023	−0.2%	0.4%
l_{11}	−0.082	−0.081	−1.4%	1.5%
l_{21}	0.013	0.009	−29.6%	9.4%
l_{12}	−0.342	−0.334	−2.5%	0.7%
l_{22}	0.014	0.007	−49.3%	45.2%

perturbation (5%) in the direct perturbation approach were neglected. The statistical uncertainties in the relative difference between GPT and reference results accounts for sum of the variance of the two methods.

6. Sensitivity studies

The sensitivity coefficient analysis allows a detailed understanding of the coupling phenomena. Some examples will be given in this paragraph, related to the model coupled reactor of Fig. 3. As shown above in Fig. 4, the flux radial distributions by energy band have been calculated as well as the fission rate weighted spectra in the two fissile regions, and they provide the basis for understanding the physics of the sensitivity analysis. In fact a number of perturbations were analyzed, e.g. the variation of the hydrogen density in Reactor 2 or of the boron content in the filter region (see Fig. 3). ^{238}U individual cross sections have also been considered.

In fact, as an example, a higher H density in the thermal spectrum region, increases, as expected, the k_{22} as indicated in Table 2. It also increases the coupling effect represented by k_{21}, since fast neutrons coming from the fast spectrum region will have more probability of slowing down to thermal energies where the ^{235}U fission cross section increases. On the contrary, the well thermalized neutrons in region 2 will have more probability to be captured (because of higher capture cross section) by the B-10 in the filter and, consequently, the coupling coefficient k_{12} will decrease.

The decrease of the S1/S2 ratio is also expected, in view of the enhanced role of the thermal region in terms of power share, which is shown in Fig. 5.

The effect of the variation of the boron content in the filter has smaller effects as shown by the sensitivity coefficients of Table 3 (e.g. the increase of 5% of the boron content induces only ~1% decrease of the coupling coefficients k_{12} or k_{21}). The effect on the power share is even smaller.

As for the coupling coefficient k_{21}, which accounts for neutrons born in the fast neutron region and giving fission in the thermal spectrum region, the sensitivity profiles of Fig. 6 indicate that the k_{21} decreases both as a consequence of an increase of the low energy absorptions of H (in the "thermal" zone) and of an increase of the filter ^{10}B total cross section at high energy. On the contrary, an increase of the H elastic cross section increases the thermalisation of the fast neutrons, increasing their contributions to the fission in the thermal spectrum zone.

As an example of individual cross sections impact on the coupling parameters, Fig. 7 indicates that any increase of the inelastic cross section of ^{238}U at very high energy (>2–3 MeV) brings neutrons to the high flux region (~100 keV–1 MeV), increasing the probability of leakage towards the thermal region, i.e. the k_{21} increases. On the contrary, an increase of the same cross section at energies below ~1 MeV, will reduce the number of neutrons able to reach the thermal spectrum region, i.e. the k_{21} decreases.

In the same figure the effects of the ^{238}U fission spectrum are also shown. They indicate an opposite trend with respect to the inelastic cross section variation: in fact e.g. an increase of the fission spectrum in the energy region below ~1 MeV means "useful (for k_{12}) neutron production", whereas an increase of the inelastic cross section in that same energy region means "useful (for k_{12}) neutron disappearance". Lastly, the total effects accounts also for the total absorption and the elastic scattering variations, that further contribute e.g. to the "useful (for k_{12}) neutron disappearance" below ~1–2 MeV.

Finally, Fig. 8 shows that increasing the boron absorption in the filter zone has the effect of decreasing the ratio R_I = (integral flux in the range 100 eV < E < 100 keV)/(total flux) due to the intermediate born absorptions and of decreasing even more the ratio R_T = (integral flux below 100 eV)/(total flux) due to the very high absorption rate of neutron born in that energy range. Such a type of indications can help to optimize e.g. the filter composition for specific objectives.
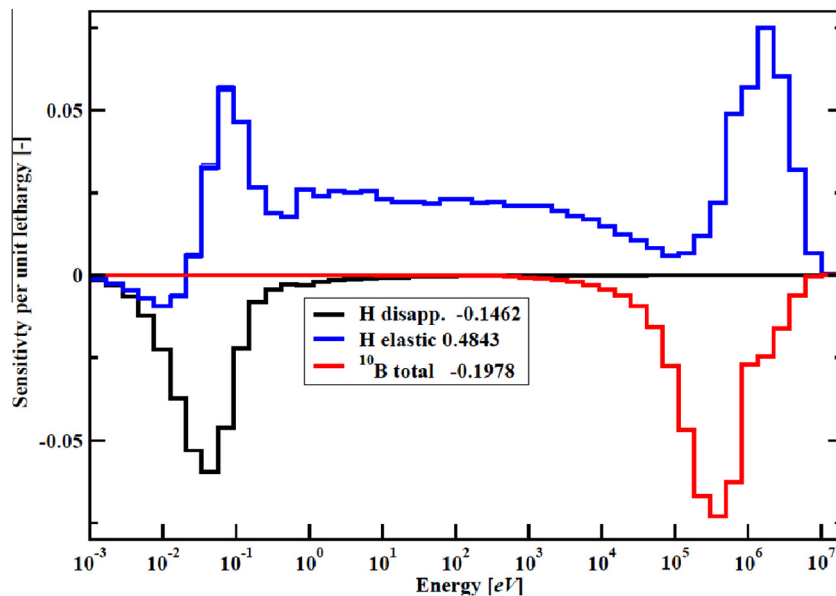

Fig. 6. Extended SERPENT-2 GPT calculations of k_{21} sensitivity to Hydrogen and Boron cross sections.
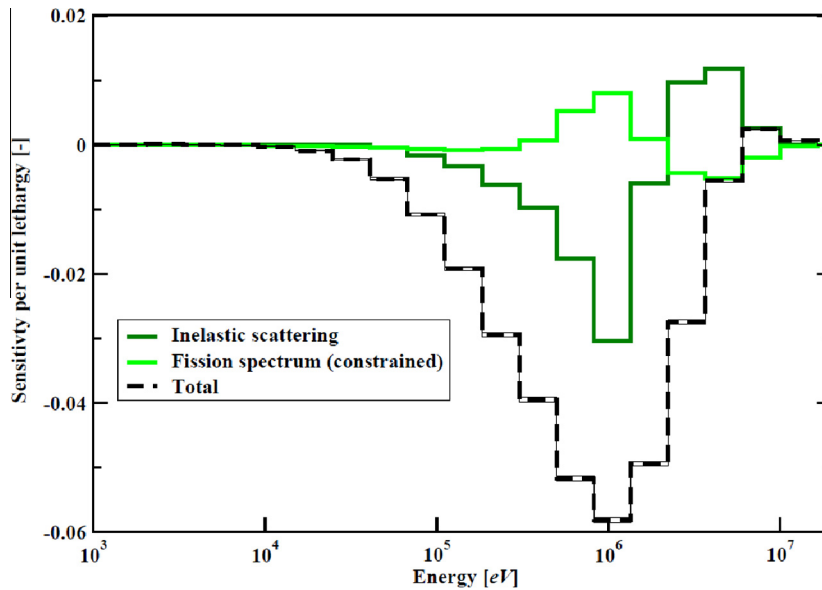
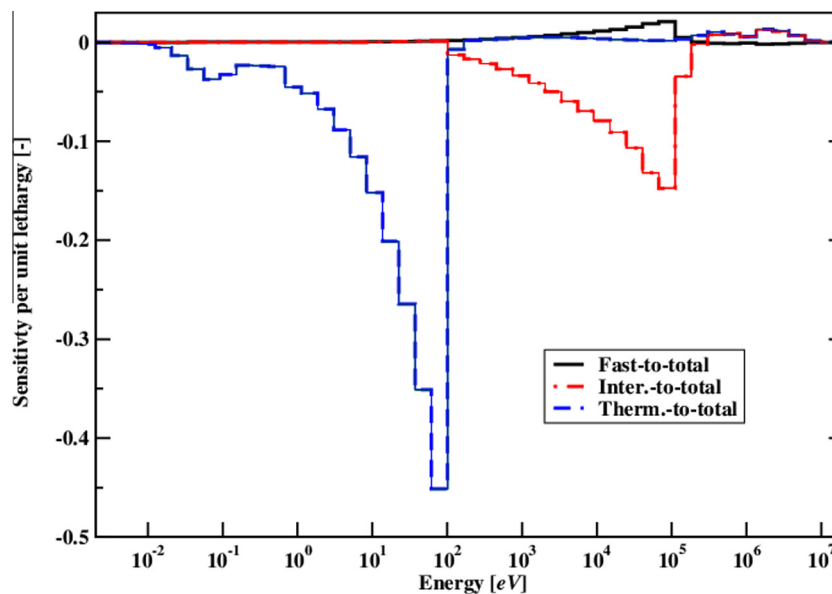**Fig. 7.** Extended SERPENT-2 GPT calculations of k_{21} sensitivity to ^{238}U cross sections.

Fig. 8. Extended SERPENT-2 GPT B$_4$C filter zone. Spectral indexes sensitivity to ^{10}B disappearance ((n,α) + (n,γ)) cross sections.

These sensitivity analyses can be of interest also in cases of large cores with significant coupling effects, as indicated previously. The modified SERPENT code will then be a particularly useful tool of analysis.

7. Conclusions

Coupled reactors and the coupling features of large or heterogeneous core reactors can be investigated with the Avery's theory that allows a physics understanding of the main features of these systems. However, the complex geometries that are often encountered in association with coupled reactors, require a detailed geometry description that can be easily provided by modern Monte Carlo (MC) codes. This implies a MC calculation of the coupling parameters defined by Avery and of the sensitivity coefficients that allow further detailed physics analysis. The results presented in this paper show that the MC code SERPENT has been successfully modified to meet the required capabilities.

Future work will address the analysis of the key issue of power shape potential tiltness in coupled systems, using the relation between Boltzmann equation eigenvalue separation and Avery coupling coefficients.

References

Abramov, B.D., 2001. Modifications to the theory of coupled reactors. At. Energy 90 (5).

Aufiero, M. et al., 2015. A collision history-based approach to sensitivity/perturbation calculations in the continuous energy Monte Carlo code SERPENT. Ann. Nucl. Energy 85, 245–258.

Avery, R.L., 1958. Theory of coupled reactors. In: Proc. 2nd Int. Conf. Peaceful Uses of At. Energy, vol. 12, p. 182.

Baldwin, G.C., 1959. Kinetics of a reactor composed of two loosely coupled cores. Nucl. Sci. Eng. 6, 320.

Bustraan, M., et al., 1970. STEK, the Fast-Thermal Coupled Facility of RCN at Petten, RCN-122.

Carney, S.E., Brown, F.B., Kiedrowski, B.C., Martin, W.R., 2012. Fission Matrix Capability for MCNP Monte Carlo. Los Alamos National Laboratory, LA-UR-12-24533.

Komata, M., 1969. On the derivation of Avery's coupled reactor kinetics equations. Nucl. Sci. Eng. 38, 193.

Kukharchuk, O.F., et al., 2000. Coupled fast-thermal system: theory and experiments. In: Proc. Int. Conf. PHYSOR 2000.

Laureau, A., et al., 2015. Coupled neutronics and thermal-hydraulics transient calculations based on a fission matrix approach: application to the molten salt fast reactor. In: ANS MC2015 – Joint International Conference on Mathematics and Computation (M&C), Supercomputing in Nuclear Applications (SNA) and the Monte Carlo (MC) Method, Nashville, Tennessee, April 19–23, 2015.

Leppänen, J. et al., 2014. Calculation of effective point kinetics parameters in the SERPENT 2 Monte Carlo code. Ann. Nucl. Energy 65, 272–279.

Meister, H., et al., 1964. The Karlsruhe Fast-Thermal Argonaut Reactor Concept, KFK-217.

Palmiotti, G., Salvatores, M., et al., 2016. Spatial effects of neutron coupling/decoupling in different types of reactors and impact on neutronics performances. Ann. Nucl. Energy.

Rimpault, G., et al., 2002. The ERANOS code and data system for fast reactor neutronic analyses. In: Proc. Physor 2002 Conference, Seoul (Korea), October 2002.

Seale, R.L., 1964. Coupled Core Reactors, LAMS-2967.

Sen, S., et al., 2016. A versatile innovative thermal-fast coupled test reactor. In: Proc. Physor 2016 Conference, Sun Valley, Idaho, (USA), May 2016.

Toppel, B.J., 1957. The Coupled Aspects of a Fast-Thermal Critical: ZPR-V, ANL-5775.

Frédéric Varaine et al., 2012. Pre-conceptual design study of ASTRID core. In: Proceedings of ICAPP'12, Chicago, USA, June 24–28, 2012.